Electronic Supplementary Material (ESI) for Journal of Materials Chemistry A.

Electronic Supplementary Information

Optimizing semiconductor thin films with smooth surfaces and well-interconnected networks for high-performance perovskite solar cells

Wu-Qiang Wu,[a] Dehong Chen,[a] Fuzhi Huang,[b] Yi-Bing Cheng,[c]* and Rachel A. Caruso[ad]**

[a]Particulate Fluids Processing Centre, School of Chemistry, The University of Melbourne, Melbourne, Victoria 3010, Australia.

[b]State Key Laboratory of Advanced Technology for Materials Synthesis and Processing, Wuhan University of Technology, Wuhan, 430070, China

[c]Department of Materials Science and Engineering, Monash University, Victoria 3800, Australia.

[d]CSIRO Manufacturing, Private Bag 10, Clayton South, Victoria 3169, Australia

Email: dehongc@unimelb.edu.au, rcaruso@unimelb.edu.au,

yibing.cheng@monash.edu

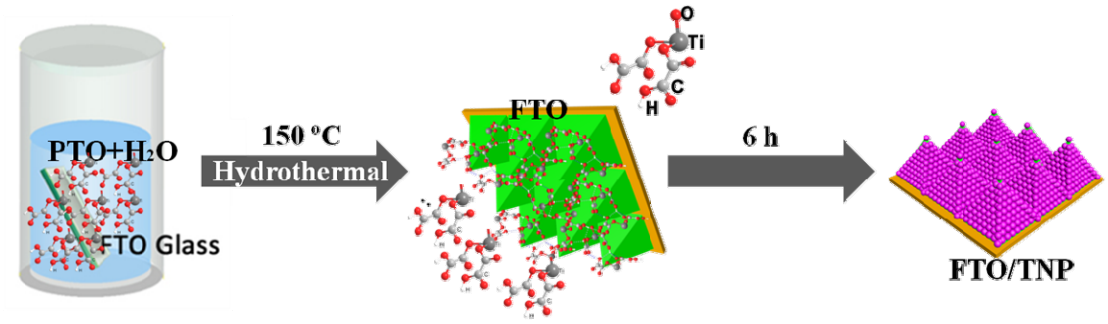

Figure S1. Schematic of the one-step hydrothermal route to fabricate TNP thin films on FTO glass, in which bare FTO was immersed face-down in a PTO aqueous solution and hydrothermally treated at 150 °C for 6 h. The Ti species attached to the FTO pyramidal surface, producing nanoparticles and thus forming the FTO/TNP film.

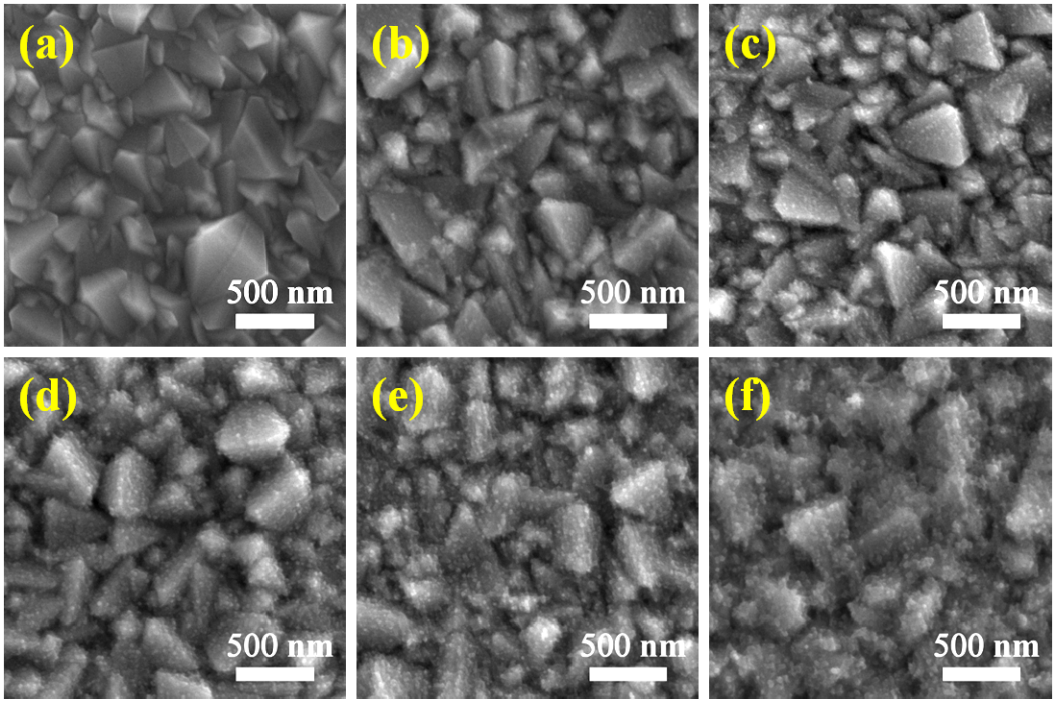

Figure S2. SEM images of the surface of FTO and the FTO/TNP substrates prepared using different PTO concentrations: (a) FTO; (b) PTO-1.7 mM; (c) PTO-3.5 mM; (d) PTO-7.0 mM; (e) PTO-14 mM; and (f) PTO-28 mM.

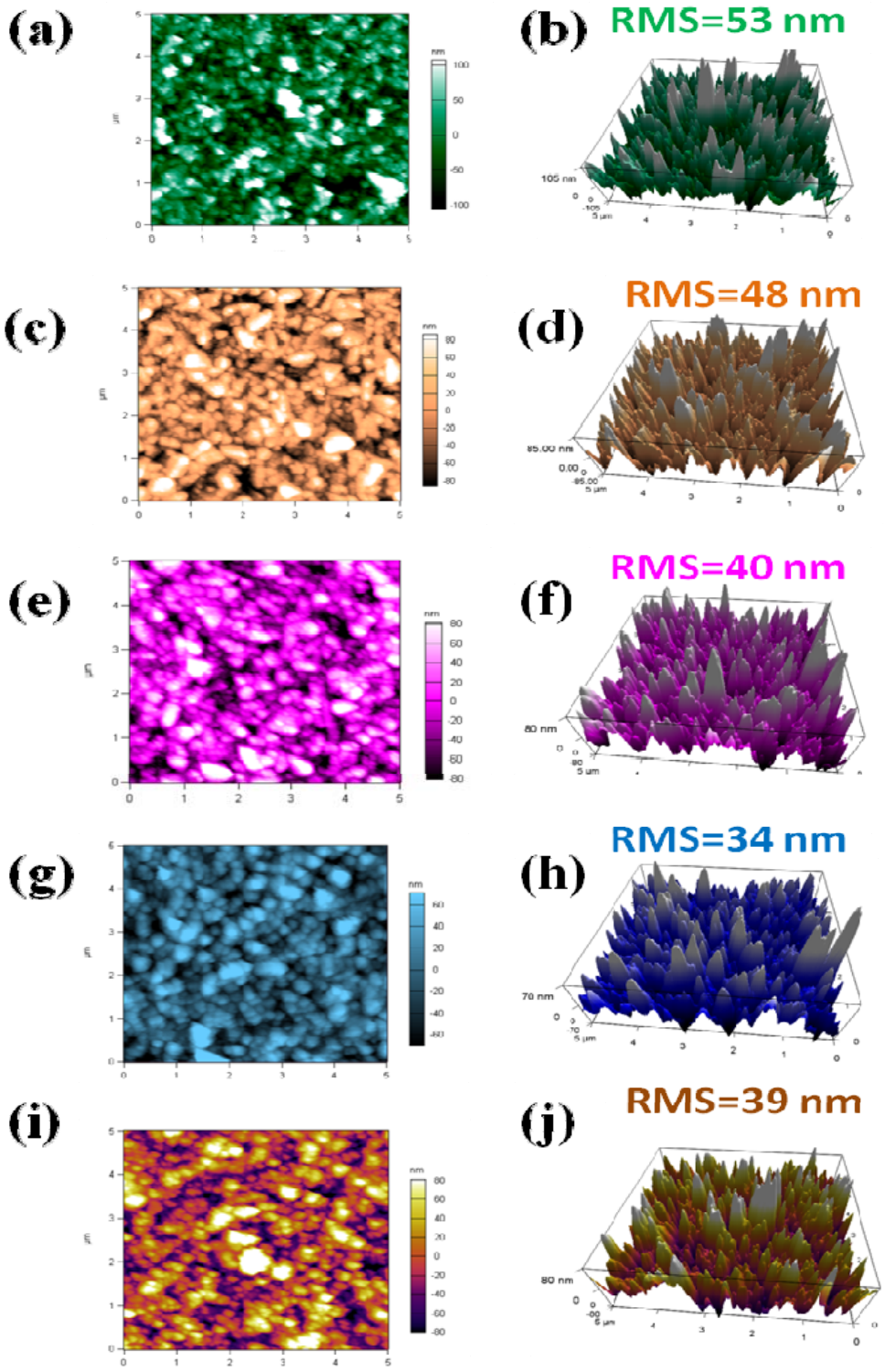

Figure S3. AFM images of the TNP coatings on FTO glass showing the roughness of the thin films prepared using different PTO concentrations: (a, b) PTO-1.7 mM; (c, d) PTO-3.5 mM; (e, f) PTO-7.0 mM; (g, h) PTO-14 mM; and (i, j) PTO-28 mM.

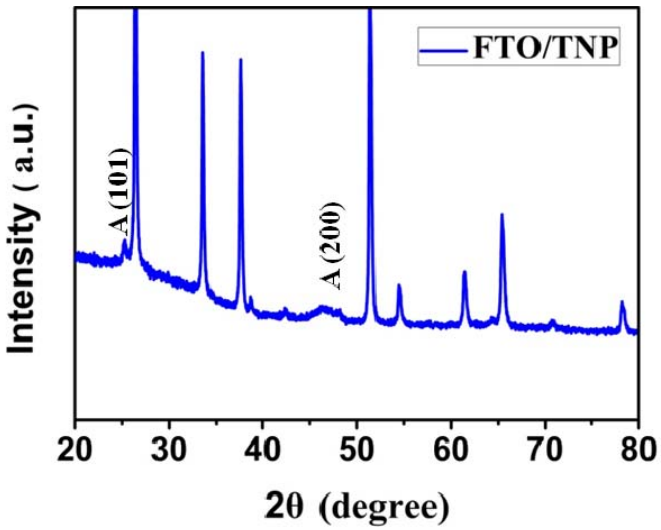

Figure S4. XRD pattern of the FTO/TNP substrate prepared using PTO-14 mM at 150 °C for 6 h via hydrothermal treatment. The two anatase peaks are labelled.

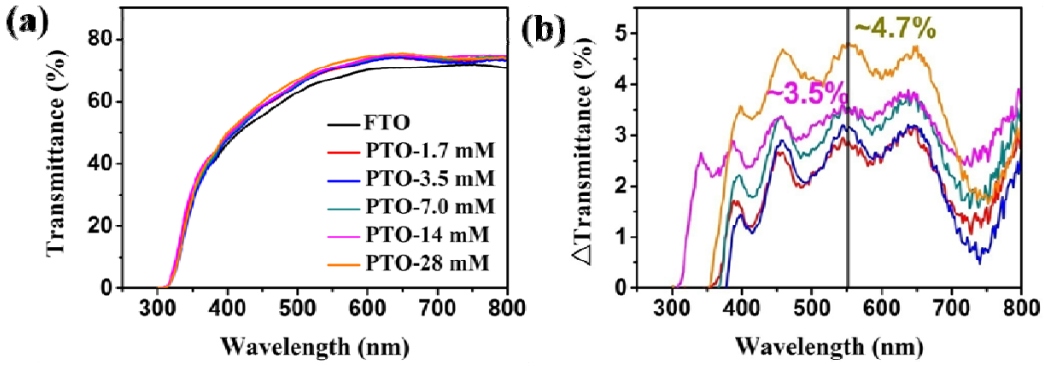

Figure S5. (a) Optical transmittance spectra of the bare FTO and FTO/TNP substrates prepared using different PTO concentrations. (b) Optical transmittance enhancement of the different FTO/TNP substrates as compared to the pristine FTO glass (same legend as (a)). For the transmittance measurement, the incident light was shone on the glass side for each sample, which is consistent with the illumination direction used to record the *J-V* curves. The improved optical transmittance of the TNP films coated on FTO glass might be related to the porosity and thickness of the titania nanostructures, which will affect the light interference and thus reflective index of the films.

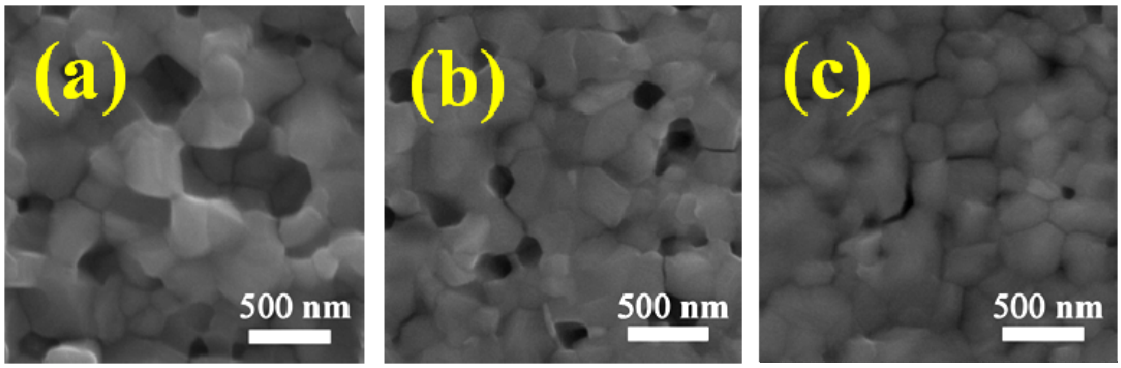

Figure S6. Top surface SEM images of the $CH_3NH_3PbI_3$ films deposited on different TNP films prepared with different PTO concentrations: (a) PTO-3.5 mM, (b) PTO-7.0 mM, and (c) PTO-28 mM.

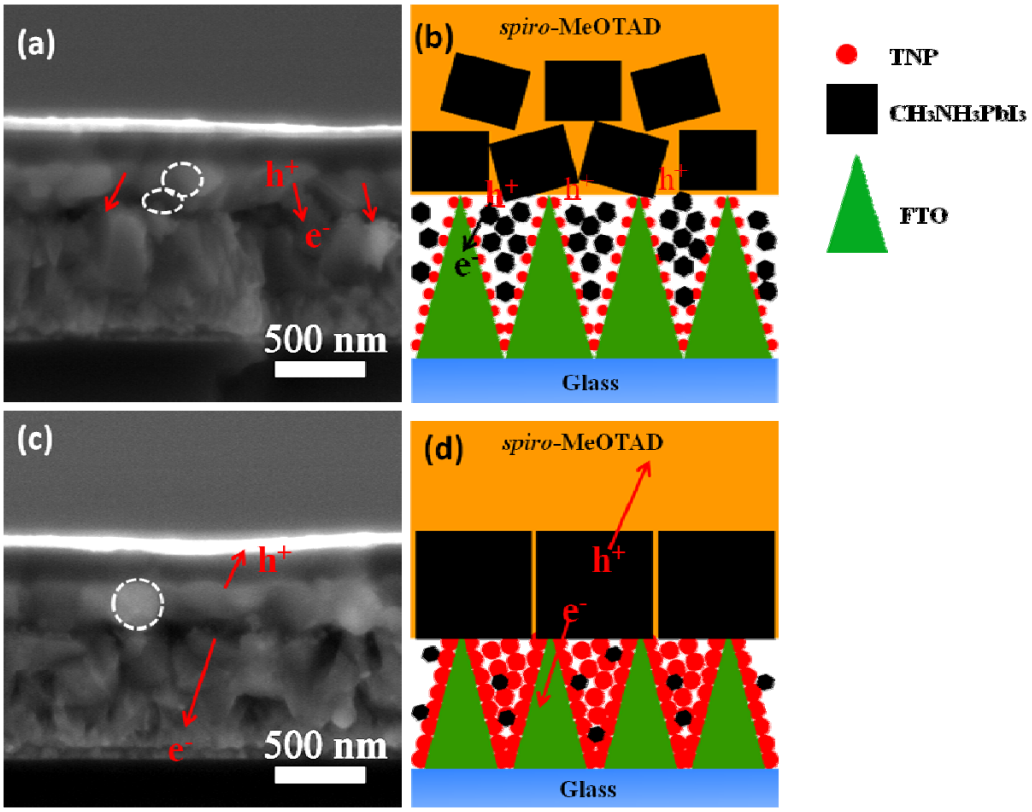

Figure S7. Cross-sectional SEM images of the PSC devices constructed using (a) PTO-1.7 mM and (c) PTO-14 mM; (b, d) Scheme of charge recombination behavior between the TNP ETL and spiro-MeOTAD HTM in TNP/Perovskite/spiro-MeOTAD films consisting of a double-layered discrete perovskite capping layer (PTO-1.7 mM) or a uniform monolayer perovskite upper layer (PTO-14 mM).

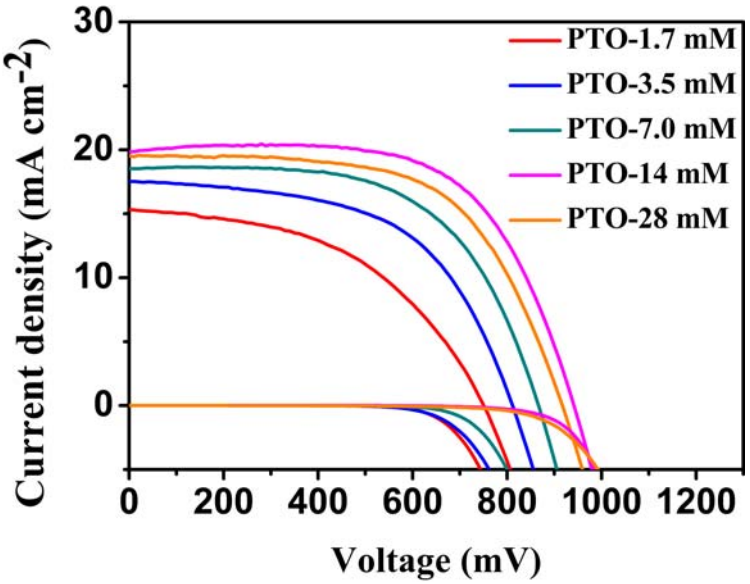

Figure S8. *J-V* curves of the PSCs constructed using the different FTO/TNP electrodes.

Table S1. Photovoltaic parameters (J_{sc}, V_{oc}, FF, and η) of the PSCs constructed using different TNP thin film ETLs under one sun illumination (AM 1.5 G, 100 mW cm^{-2}).

Cells	J_{sc} (mA cm^{-2})	V_{oc} (mV)	η (%)	*Average* η* (%)	*FF*
PTO-1.7 mM	15.31	751	5.55	5.02±0.45	0.48
PTO-3.5 mM	17.51	812	7.91	7.25±0.38	0.56
PTO-7.0 mM	18.53	866	9.61	8.96±0.40	0.60
PTO-14 mM	19.85	942	12.08	11.45±0.35	0.65
PTO-28 mM	19.55	917	10.94	9.43±0.37	0.61

[*] data for average PCE (η) are calculated from 10 devices.

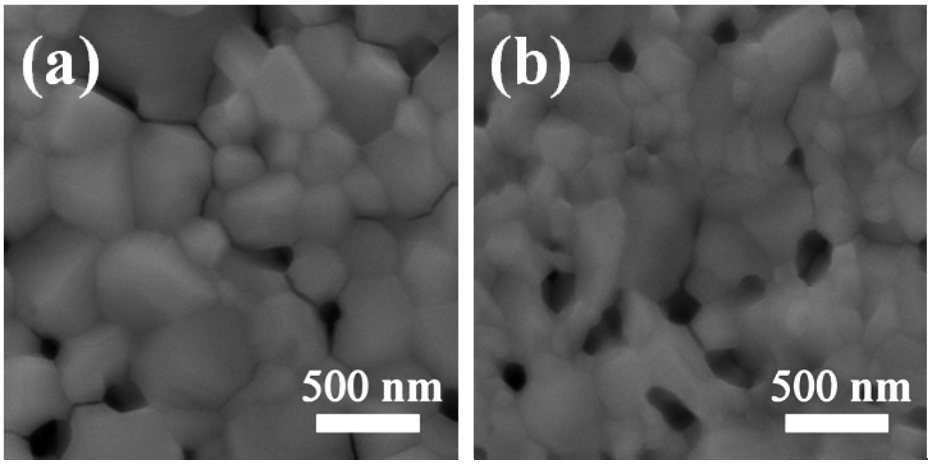

Figure S9. Top view SEM images of vapor annealed perovskite films using (a) DMF:CBZ=1:2 and (b) pure CBZ.

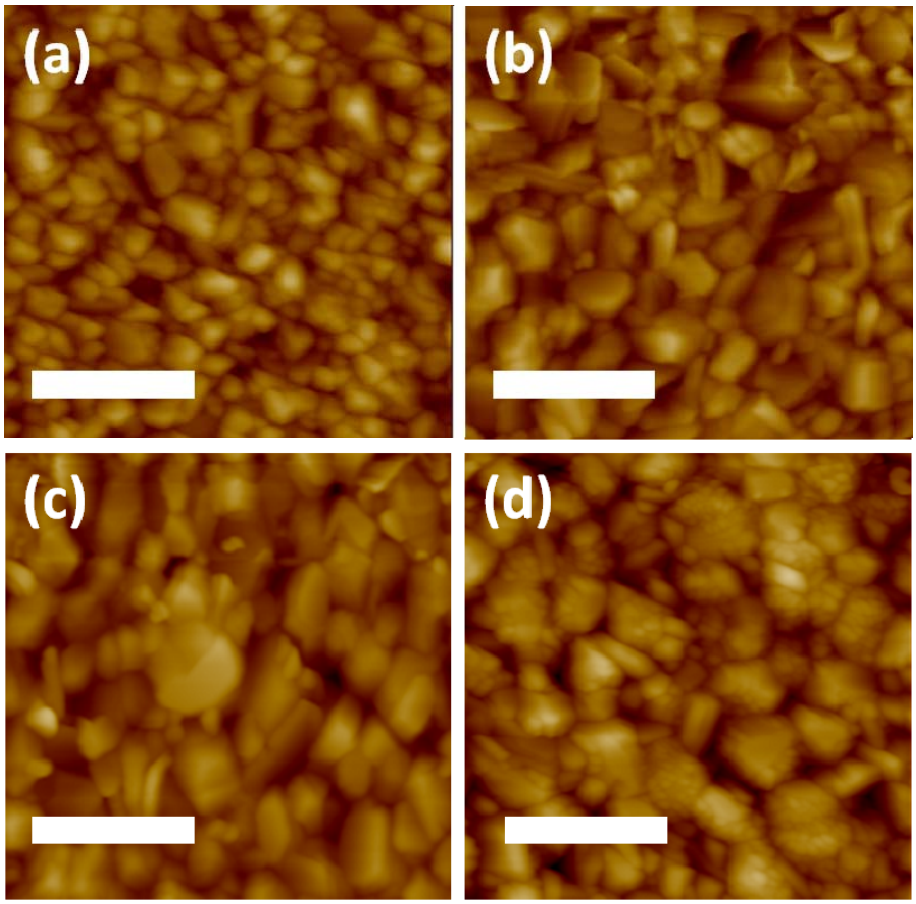

Figure S10. AFM topography of the surface of perovskite films fabricated using different vapor-assisted annealing conditions: (a) no vapor; (b) DMF; (c) DMF:CBZ=2:1; and (d) DMF:CBZ=1:1. The scale bars are 2 μm. RMS for these four films are 48, 44, 36 and 30 nm from (a) to (d).

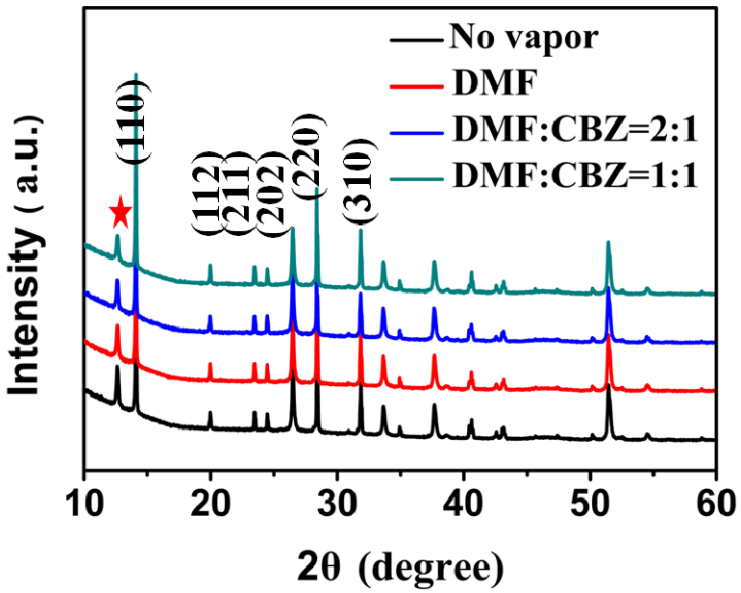

Figure S11. XRD patterns of the perovskite films fabricated under different annealing conditions, followed by seven-days storage in an ambient environment. The peak labelled with the red star represents PbI_2.

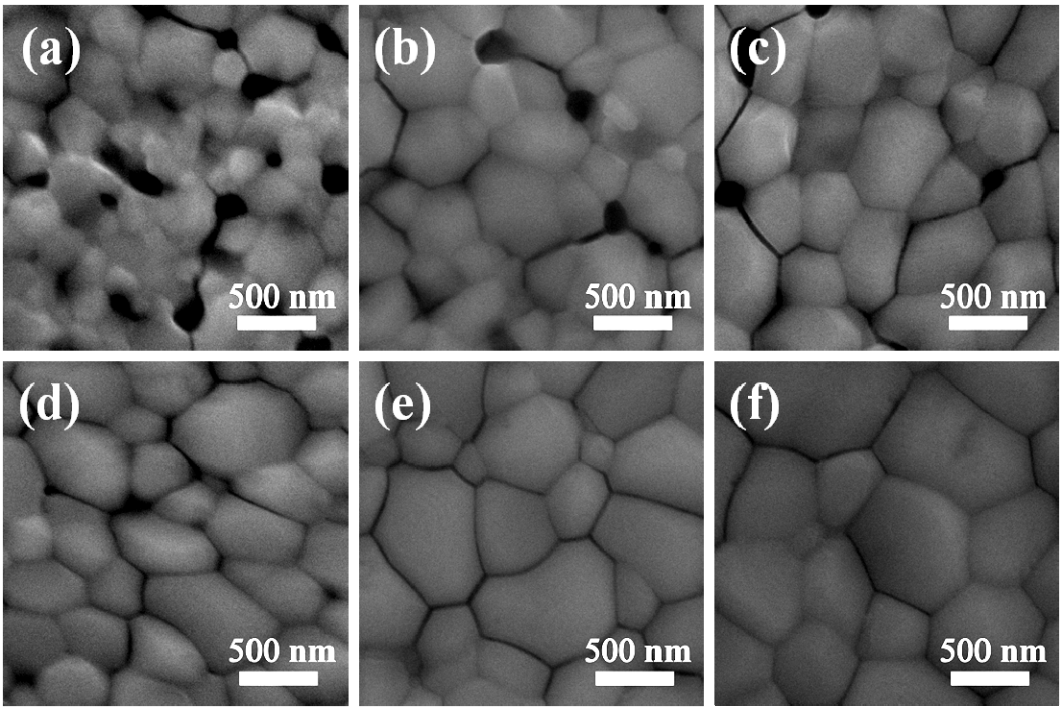

Figure S12. SEM images of the perovskite films fabricated using blended solvent vapor annealing in DMF:CBZ=1:1 for different times: (a) 1 min, (b) 5 min, (c) 10 min, (d) 20 min, (e) 30 min, and (f) 40 min, at 100 °C.

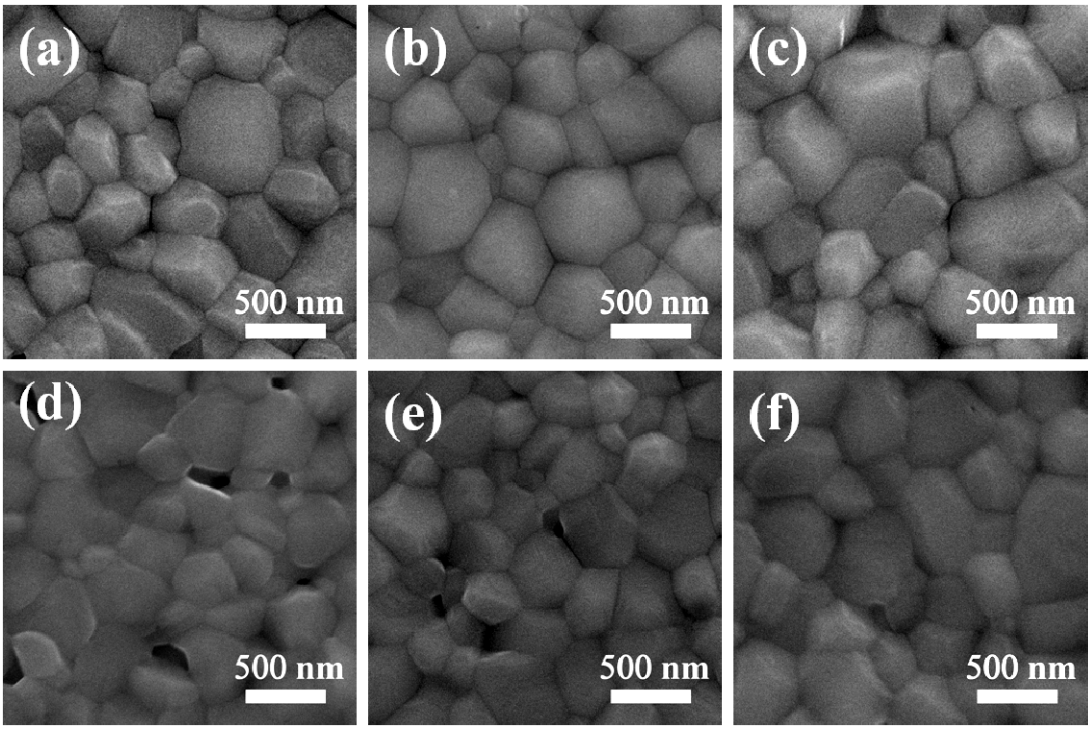

Figure S13. SEM images of the perovskite films annealed using different blended solvent compositions at 100 °C for different times: (a) 40 min, (b) 60 min, and (c) 90 min in DMF:CBZ = 2:1; (d) 60 min, (e) 90 min, and (f) 120 min in DMF:CBZ = 1:2.

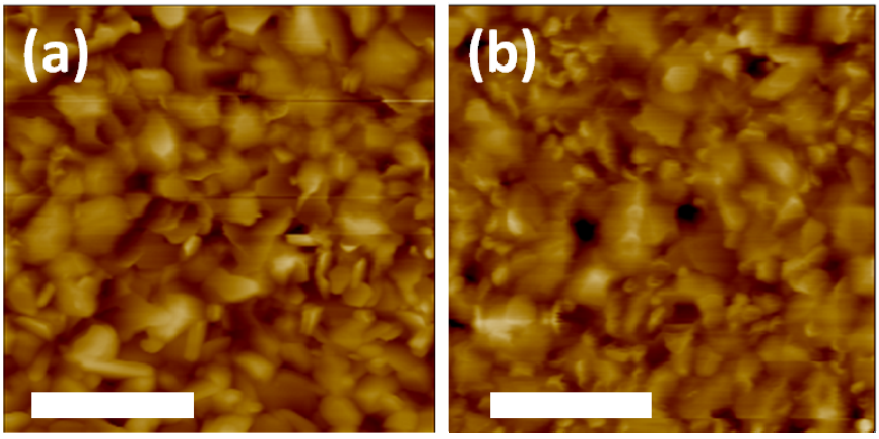

Figure S14. AFM topography of the surface of perovskite films annealed under (a) DMF:CBZ = 2:1 for 60 min and (b) DMF:CBZ = 1:2 for 120 min. The scale bars are 2 μm. RMS for these two films are (a) 32 and (b) 35 nm.

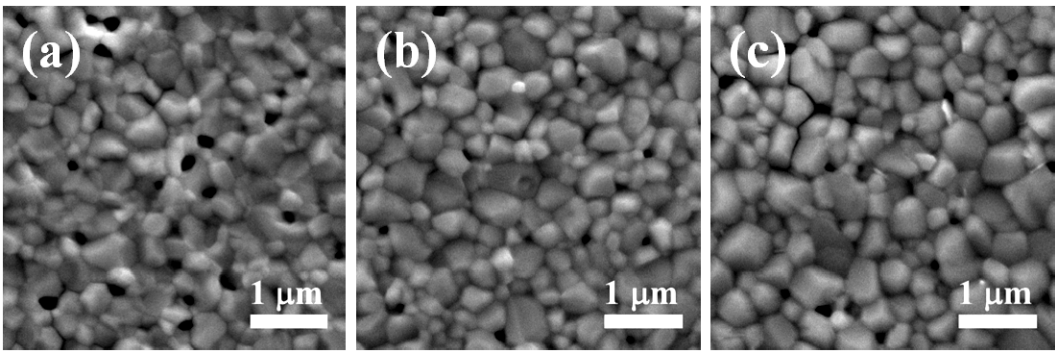

Figure S15. SEM images of solvent vapor (DMF:CBZ = 1:1) annealed perovskite films annealed at (a) 70 °C, (b) 100 °C, and (c) 150 °C for 5 min.

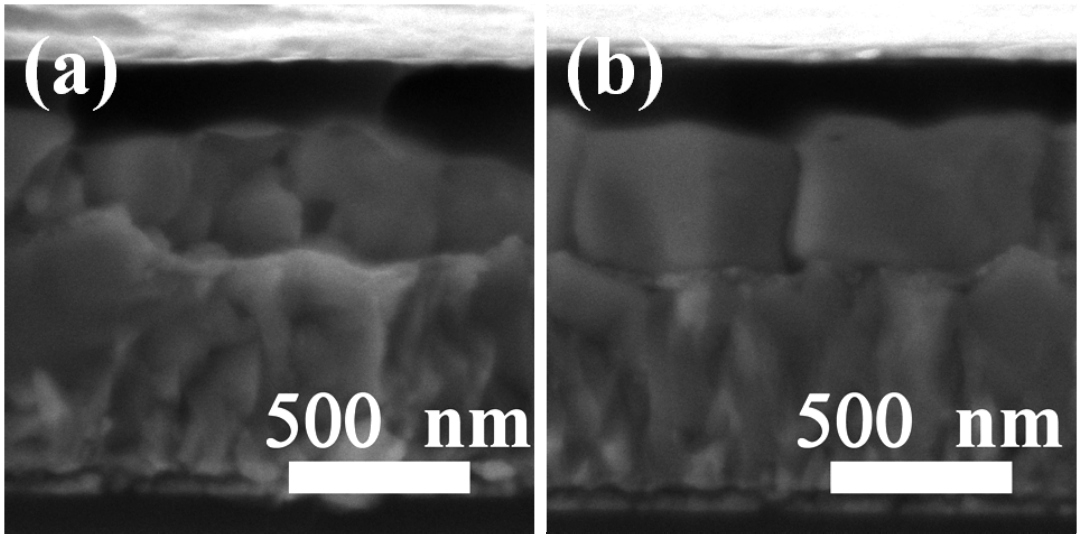

Figure S16. Cross-sectional SEM images of devices fabricated with two representative perovskite films: (a) without (no-vapor) and (b) with vapor (DMF:CBZ=1:1) annealing treatment.

Table S2 Morphological parameters of the different perovskite films annealed at 100 °C under different conditions (solvent composition and annealing time). D_1 is grain size distribution of the perovskite crystal estimated from SEM images; *RMS* is the root-mean-squared roughness of the perovskite films from AFM measurements.

Perovskite Films	***Time* (min)**	**D_1 (nm)**	***RMS* (nm)**
No vapor	10	250-500	48
DMF	30	400-750	44
DMF:CBZ=2:1	30	300-650	36
	60 (optimal)	**300-800**	**32**
DMF:CBZ=1:1	1	100-400	-
	5	200-600	-
	10	300-650	-
	20	300-750	-
	30 (optimal)	**300-850**	**30**
	40	300-1000	-
DMF:CBZ=1:2	30	150-500	-
	120 (optimal)	**300-750**	**35**

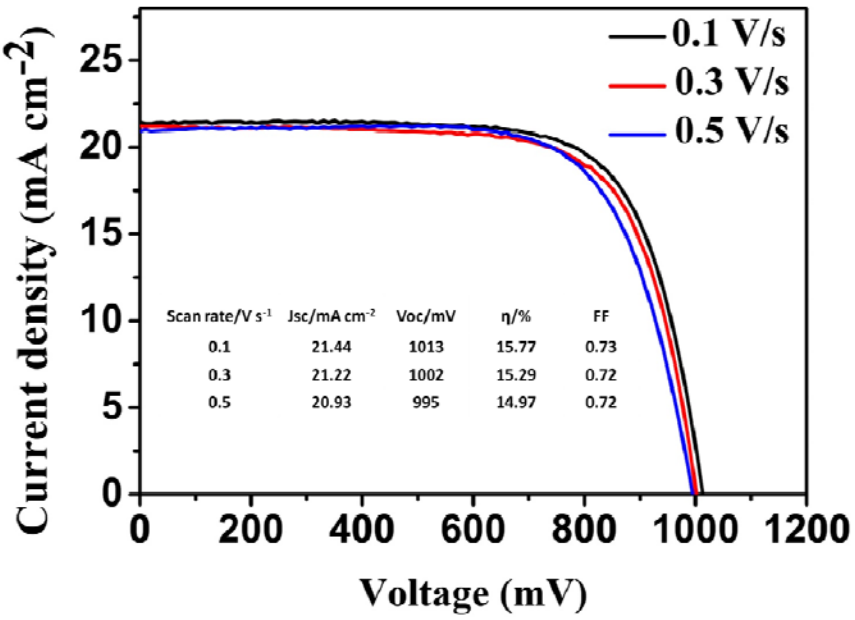

Figure S17. *J-V* characteristics of the best-performing cells (DMF:CBZ=1:1) obtained at scan rates of 0.1, 0.3 and 0.5 V s^{-1}.

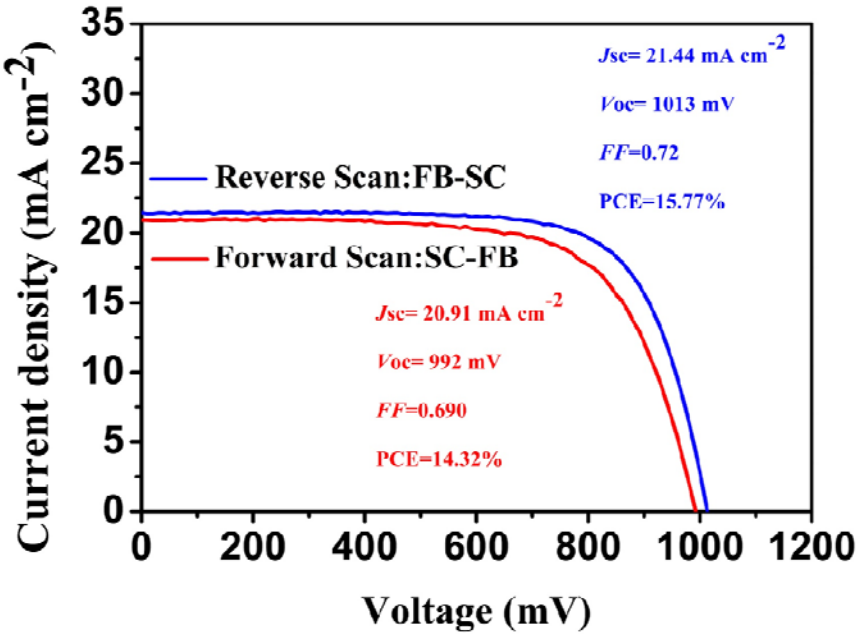

Figure S18. *J-V* curves of a device based on optimized TNP and perovskite semiconducting layers measured by forward scan (SC-FB, red line) and reverse scan (FB-SC, blue line) with a scan rate of 0.1 V s^{-1} under AM 1.5 simulated sunlight illumination.

Table S3. Photovoltaic parameters of the PSCs based on a batch of optimized TNP (PTO-14 mM) and $CH_3NH_3PbI_3$ (DMF:CBZ=1:1) thin films under one sun illumination (AM 1.5G, 100 mW cm^{-2}) showing the high reproducibility of the device performance.

Cell	J_{sc} (mA cm^{-2})	V_{oc} (mV)	η (%)	*FF*
1	20.87	1004	15.50	0.74
2	22.16	1031	15.38	0.67
3	20.56	1019	14.41	0.69
4	21.75	1014	15.26	0.69
5	***21.44***	***1013***	***15.77***	***0.73***
6	20.93	995	14.97	0.72
7	20.09	1029	14.89	0.72
8	20.69	997	15.03	0.73
9	21.31	1007	15.57	0.73
10	21.20	1043	15.75	0.71
Average	21.10±0.57	1015±15	15.25±0.41	0.71±0.02

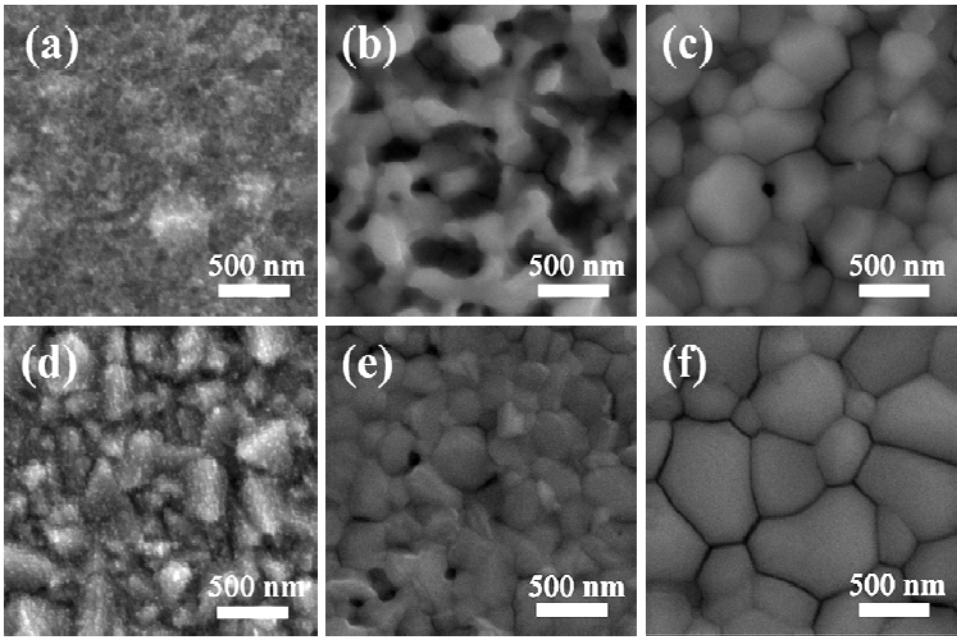

Figure S19. SEM images of the titania films obtained using reference mp-TiO_2 (a) and TNP (PTO-14 mM) (d) and the perovskite-deposited films prepared using gas-assisted spin coating on the reference mp-TiO_2 film (b) and TNP (PTO-14 mM) film (e) or gas-assisted spin coating combined with vapor-assisted annealing on the reference mp-TiO_2 film (c) and TNP (PTO-14 mM) film(f).

Table S4. Comparison of the photovoltaic parameters of the PSCs based on FTO/mp-TiO_2/$CH_3NH_3PbI_3$ and FTO/TNP/$CH_3NH_3PbI_3$ electrodes fabricated with or without vapor annealing (DMF:CBZ=1:1) under one sun illumination (AM 1.5G, 100 mW cm^{-2}).

Cell	J_{sc} (mA cm^{-2})	V_{oc} *(mV)*	η *(%)*	*FF*
mp-TiO_2	19.26	909	9.62	0.55
mp-TiO_2-vapor	20.53	937	12.17	0.63
TNP	19.85	942	12.08	0.65
TNP-vapor	21.44	1013	15.77	0.73